

1 **Diffusion NMR Study of Complex Formation in**  
2 **Membrane-Associated Peptides**

3 **Suliman Barhoum, Valerie Booth and Anand Yethiraj**

4  
5 Received: date / Accepted: date

6 **Abstract** Pulsed-field-gradient nuclear magnetic resonance (PFG-NMR) is used to obtain  
7 the true hydrodynamic size of complexes of peptides with sodium dodecyl sulfate SDS  
8 micelles. The peptide used in this study is a 19-residue antimicrobial peptide, GAD-2. Two  
9 smaller dipeptides, alanine-glycine (Ala-Gly) and tyrosine-leucine (Tyr-Leu), are used for  
10 comparison. We use PFG-NMR to simultaneously measure diffusion coefficients of both  
11 peptide and surfactant. These two inputs, as a function of SDS concentration, are then fit to  
12 a simple two species model that neglects hydrodynamic interactions between complexes.  
13 From this we obtain the fraction of free SDS, and the hydrodynamic size of complexes in a  
14 GAD-2-SDS system as a function of SDS concentration. These results are compared to those  
15 for smaller dipeptides and for peptide-free solutions. At low SDS concentrations ( $[SDS] \leq$   
16  $25 \text{ mM}$ ), the results self-consistently point to a GAD-2-SDS complex of fixed hydrodynamic  
17 size  $R = (5.5 \pm 0.3) \text{ nm}$ . At intermediate SDS concentrations ( $25 \text{ mM} < [SDS] < 60 \text{ mM}$ ), the

---

Suliman Barhoum  
Department of Physics and Physical Oceanography, Memorial University of Newfoundland, St. John's, NL,  
Canada  
E-mail: sulimanb@mun.ca,  
Valerie Booth  
Department of Biochemistry, Memorial University of Newfoundland, St. John's, NL, Canada  
Tel.: 709-864-4523  
E-mail: vbooth@mun.ca,  
Anand Yethiraj  
Department of Physics and Physical Oceanography, Memorial University of Newfoundland, St. John's, NL,  
Canada  
Tel.: 709-864-2113  
E-mail: ayethiraj@mun.ca

18 apparent size of a GAD-2-SDS complex shows almost a factor of two increase without a  
19 significant change in surfactant-to-peptide ratio within a complex, most likely implying  
20 an increase in the number of peptides in a complex. For peptide-free solutions, the self-  
21 diffusion coefficients of SDS with and without buffer are significantly different at low SDS  
22 concentrations but merge above  $[SDS]=60$  mM. This concentration is identified as an onset  
23 of crowding beyond which it is impossible, even in principle, to extract information about  
24 hydrodynamic size of the peptide-surfactant complex.

25 **Keywords** Antimicrobial peptide · Peptide-micelle complexes · NMR diffusometry · NMR  
26 relaxometry

## 27 Introduction

28 Membrane-associated proteins and peptides are often studied in a micellar environment  
29 (Tulumello and Deber, 2009; Sanders and Sönnichsen, 2006). Like membrane bilayers, mi-  
30 celles provide a hydrophobic-hydrophilic interface, but unlike them, they are small enough  
31 to enable solution NMR signals to be observed. Micelles are commonly employed in NMR  
32 structure determination of membrane proteins (Qureshi and Goto, 2012; Tulumello and  
33 Deber, 2009), but have also been used in studies where the protein-lipid interaction itself is  
34 the focus (Cozzolino et al, 2008; Morein et al, 1996; Yu et al, 2006; Romani et al, 2010). NMR-  
35 based techniques have been utilized to study an important class of membrane-associated  
36 proteins that are called antimicrobial peptides (AMPs).

37 AMPs are often short peptides consisting of 12 to 50 residues and act by interacting  
38 with (and often disrupting) membranes. AMPs have been shown to play an important  
39 role in attacking and killing microbes such as bacteria, viruses, and fungi (Zasloff, 2002;  
40 Nicolas, 2009; Hoskin and Ramamoorthy, 2008; Chinchar et al, 2004). Moreover, some AMPs  
41 exhibit activity against tumor cells in a mammal's body by disrupting the membrane of the  
42 diseased cells and targeting the cell interior without affecting the membrane of host cells  
43 (Rege et al, 2007). This selectivity, for microbial and/or tumor cells, is thought to arise due  
44 to the amphiphilic structure of the AMP that has an affinity to the lipid bilayer structure of

45 the microbial cells as well as due to the interaction between the positive charge on the AMP  
46 with the anionic components of the tumor or pathogen cell membrane (Epanand and Vogel,  
47 1999). Therefore, anionic sodium dodecyl sulfate SDS surfactant micelles are commonly  
48 employed in the structural studies of AMPs, as well as other membrane proteins (Wang,  
49 2008, 1999; Whitehead et al, 2001; Orfi et al, 1998; Begotka et al, 2006; Deaton et al, 2001;  
50 Whitehead et al, 2004; Gao and Wong, 1998; Buchko et al, 1998).

51 A knowledge of the hydrodynamic size of proteins plays an important role in un-  
52 derstanding their conformations (Jones et al, 1997). This is also the case for peptides in  
53 peptide-micelle complexes, where there could be many coexisting conformations. The hy-  
54 drodynamic size of complexes can be obtained by measuring diffusion coefficients and  
55 using the Stokes-Einstein-Sutherland equation  $R_H = K_B T / 6\pi\eta D_o$ . This approach, however,  
56 is only strictly valid when the self-diffusion coefficient  $D_o$  is obtained by measuring the  
57 diffusion coefficient as a function of the surfactant concentration and then extrapolating to  
58 infinite dilution. Such a procedure is often not practical when the amount of peptide or pro-  
59 tein is limited in quantity. As a result of this, "apparent" hydrodynamic radii are routinely  
60 reported, without such extrapolation, in systems with rather large surfactant concentrations  
61 (Binks et al, 1989; Gimel and Brown, 1996; Sarker et al, 2011).

62 An important phenomenon to consider with respect to large macromolecular concen-  
63 trations is crowding. Macromolecular crowding refers to the non-specific excluded volume  
64 (steric) effect of macromolecules with respect to one another in an environment where the  
65 macromolecular volume fraction  $\Phi$  is large; an example is a living cell with  $\Phi=40\%$  (Zhou  
66 et al, 2008). At finite dilutions there are hydrodynamic corrections to diffusion (Batchelor,  
67 1976) even for a simple colloidal system of spherical particles. It is now being realized  
68 that electrostatic and hydrodynamic interactions sensitively affect macromolecular dynam-  
69 ics (Zhou et al, 2008; Schreiber et al, 2009).

70 The nature of the association of peptides with anionic SDS micelles depends on the  
71 details of the electrostatic environment; for example, cationic peptides bind more strongly  
72 than their zwitterionic counterparts (Begotka et al, 2006). NMR diffusometry studies have  
73 found that peptide binding with anionic SDS micelles and zwitterionic dodecylphospho-

74 choline (DPC) micelles are different, also due to the difference in electrostatic environment  
75 (Whitehead et al, 2004). Similarly, it was found that a cell-penetrating peptide (CPP) al-  
76 ters the dynamics and size of neutral and negatively charged bicelles in different ways  
77 (Andersson et al, 2004).

78 PFG-NMR studies have shown that the hydrophobic interaction can play a signifi-  
79 cant role on the binding of peptides and tripeptides to micelles (Deaton et al, 2001; Orfi  
80 et al, 1998), as well as neuropeptides to a membrane-mimic environment (Chatterjee et al,  
81 2004). NMR studies were also carried out to explore the binding of a neuropeptide to  
82 SDS micelles in the presence of zwitterionic 3-[(3-cholamidopropyl) dimethylammonio]-  
83 1-propanesulfonate (CHAPS) surfactant as a crude model for cholesterol in the biological  
84 membrane. These studies showed that having comicelles composed of SDS and CHAPS sur-  
85 factants inhibits the hydrophobic interaction of the neuropeptide with the core of comicelles  
86 (Whitehead et al, 2001).

87 Since AMPs are subjects of much interest and also represent an even larger class of  
88 amphipathic, helical peptides, a helical AMP, GAD-2, was selected for this study. GAD-2  
89 and a related peptide, GAD-1, have been identified in recent efforts to discovery new AMPs  
90 (Fernandes et al, 2010; Browne et al, 2011; Ruangsri et al, 2012). In this work, we used NMR  
91 diffusometry and relaxometry to study the interaction between the cationic GAD-2 AMP  
92 and an anionic SDS micelle as a membrane mimic environment. In order to do so, we use  
93 a simple mathematical model that is utilized to signal the changes in the nature of the  
94 macromolecular complexes in a system of nonionic polymer-anionic surfactant system in  
95 aqueous solution (Barhoum and Yethiraj, 2010). We compare the nature of the resulting  
96 peptide-SDS complex with those that form with two much smaller peptides, and are able  
97 to identify important distinguishing characteristics. We find, reassuringly, that the most  
98 minimal model to extract hydrodynamic size works well for peptides, at least for those  
99 with the size (19 residues) of GAD-2; however, one must be careful to avoid the onset of  
100 crowding in order to reliably use these simple models.

## 101 1 Materials and Methods

102 GAD-2 peptide with average molecular mass  $M_w=2168$  g/mole was synthesized using solid  
103 phase chemical synthesis employing O-fluorenylmethoxycarbonyl (Fmoc) chemistry, on  
104 a CS336X peptide synthesizer (C S Bio Company, Menlo Park, CA) following the man-  
105 ufacturer's instructions. The peptides were synthesized at a 0.2 mmol scale with a single  
106 coupling, using prederivatized Rink amide resin. Resin and all Fmoc amino acids were pur-  
107 chased from C S Bio Company Organic solvents and other reagents used for the synthesis  
108 and purification were high- performance liquid chromatography (HPLC) grade or better  
109 and purchased from Fisher Scientific (Ottawa, ON) and Sigma-Aldrich Canada (St. Louis,  
110 MO). Deprotection and cleavage of the peptides from the resin were conducted with a  
111 trifluoroacetic acid (TFA)/water (95:5 by volume) cleavage cocktail followed by cold precip-  
112 itation with tert-butyl ether. The crude products were purified by preparative reverse-phase  
113 HPLC in a Vydac C-8 column by use of a water/acetonitrile linear gradient with 0.1% TFA  
114 as the ion pairing agent. The molecular weights of the peptides were confirmed by matrix-  
115 assisted laser desorption ionization time of flight (MALDI-TOF) mass spectrometry. The  
116 purified peptides were lyophilized and stored at 4 °C.

117 Ala-Gly peptide with  $M_w=146.14$  g/mole, Tyr-Leu peptide with  $M_w=294.35$  g/mole, and  
118 SDS (99% purity) with  $M_w=288.38$  g/mole were purchased from Sigma-Aldrich Canada  
119 (St. Louis, MO) and were used as received without further purification. Deuterium oxide  
120 D<sub>2</sub>O with 99.9% isotopic purity was purchased from Cambridge Isotope Laboratories (St.  
121 Leonard, Quebec).

**Table 1** Sample nomenclature. All samples were made with D<sub>2</sub>O as a solvent, and unless stated have 0.1 M sodium oxalate buffer in them. Final concentrations [SDS] were achieved by mixing different stock solutions. The molar ratio  $R = [\text{peptide}]/[\text{SDS}] = 30$  was kept constant for GAD-2 solutions.

Abbreviation	Final [SDS]
SDS-buf	2-187 mM
GAD-2-SDS	1-80 mM
Ala-Gly-SDS	2-60 mM
Tyr-Leu-SDS	2-60 mM

122 GAD-2-SDS, Ala-Gly-SDS, Tyr-Leu-SDS, and SDS samples were prepared with compo-  
 123 sitions according to table 1. The molar ratio (R) of SDS concentration to peptide concentra-  
 124 tion in GAD-2-SDS samples was held constant ( $R = [\text{SDS}]/[\text{GAD-2}] = 30$ ). The concentration  
 125 of dipeptides (Ala-Gly and Tyr-Leu) in Ala-Gly-SDS and Tyr-Leu-SDS systems was 2 mM.  
 126 The pH value for all samples was adjusted to be 4 by the addition of sodium deuterioxide  
 127 or deuterium chloride. All samples were made with D<sub>2</sub>O as solvent and, unless otherwise  
 128 stated, have 0.1 M sodium oxalate buffer (Na<sub>2</sub>C<sub>2</sub>O<sub>4</sub>) in them. Sodium oxalate buffer was  
 129 used in previous NMR studies to adjust the pH of SDS micelle-peptide solutions (Orfi et al,  
 130 1998; Deaton et al, 2001). It is effective as a buffer for pH below 5, where the histidine-rich  
 131 GAD-2 peptide is expected to have a net positive charge. Moreover, the chemical structure  
 132 of sodium oxalate does not include protons in it. As a result, the one dimensional proton  
 133 NMR spectra do not include buffer peaks that might overlap with SDS and peptides peaks.

134 The self-diffusion measurements were carried out in a diffusion probe (Diff30) and with  
 135 maximum field gradient (1800 G/cm) at a resonance frequency of 600 MHz on a Bruker  
 136 Avance II spectrometer. Diffusion was measured with a pulsed-field gradient stimulated-  
 137 echo sequence (Price, 1997) with (almost square) trapezoidal gradient pulses. The diffusion  
 138 coefficient of a molecule in aqueous solution is obtained from the attenuation of the signal  
 139 according to the equation (Price, 1997)

$$\ln\left(\frac{S(k)}{S(0)}\right) = -Dk \quad (1)$$

140 where  $S(k)$  is the "intensity" of the signal (the integration of the relevant peak region)  
 141 in the presence of field gradient pulse,  $S(0)$  is the intensity of the signal in the absence  
 142 of field gradient pulse,  $k = (\gamma\delta g)^2(\Delta - \delta/3)$  is a generalized gradient strength parameter,  
 143  $\gamma = \gamma^H = 2.6571 \times 10^8 \text{ T}^{-1}\text{s}^{-1}$  is the gyromagnetic ratio of the <sup>1</sup>H nucleus,  $\delta = 2 \text{ ms}$  is the  
 144 duration of the field gradient pulse,  $\Delta = 100 \text{ ms}$  is the time period between the two field  
 145 gradient pulses, and  $g$  is the amplitude of the field gradient pulse. T<sub>1</sub> relaxation mea-  
 146 surements were also performed using the Diff30 diffusion probe and the relaxation rates  
 147 ( $R_1 = 1/T_1$ ) are reported in section 2.1.

## 148 2 Results and Discussion

149 Complementary NMR-based techniques were utilized in order to identify components for  
150 different samples based on their one-dimensional NMR spectra and to extract parameters  
151 such as self-diffusion coefficients and longitudinal relaxation rates. The one-dimensional  
152 (1D) proton NMR spectra at a resonance frequency of 600 MHz on a Bruker Avance II  
153 spectrometer and at sample temperature 298 K are shown in figure 1. In all cases the trace  
154 signal of HDO in D<sub>2</sub>O is the most dominant peak (at  $\approx 4.7$  ppm); however the HDO, peptide  
155 and SDS peaks are all spectrally separable.

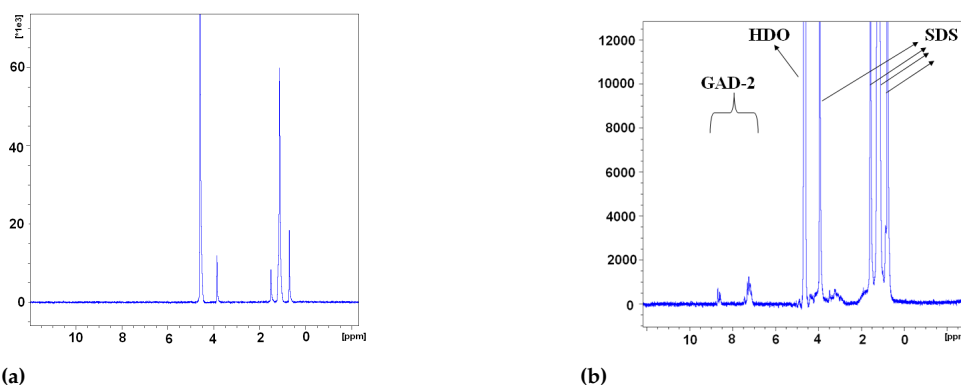


**Fig. 1** 1D <sup>1</sup>H NMR spectrum for (a) a peptide-free SDS sample with [SDS] = 6 mM (b) a GAD-2-SDS sample with [SDS]=60 mM and [GAD-2]=2 mM. Sample temperature is 298 K.

156 In this work, we carried out experiments with peptide at varying SDS concentrations  
157 in the presence of sodium oxalate buffer. We also performed experiments on pure SDS  
158 solutions as well as buffered SDS solutions for comparison. Figure 2 shows the signal at-  
159 tenuation and the self-diffusion coefficients for SDS and peptides in a buffered peptide-free  
160 SDS sample and GAD-2-SDS sample. The signal attenuation in all samples was observed  
161 to be monoexponential. This suggests that the exchange of SDS molecules between the SDS  
162 in micelles and in free solution must be very rapid in the NMR time scale. The values of  
163 the observed diffusion coefficients were calculated from the monoexponential decays using  
164 equation 1. For peptide-free SDS solutions prepared with sodium oxalate buffer (figure 2a),

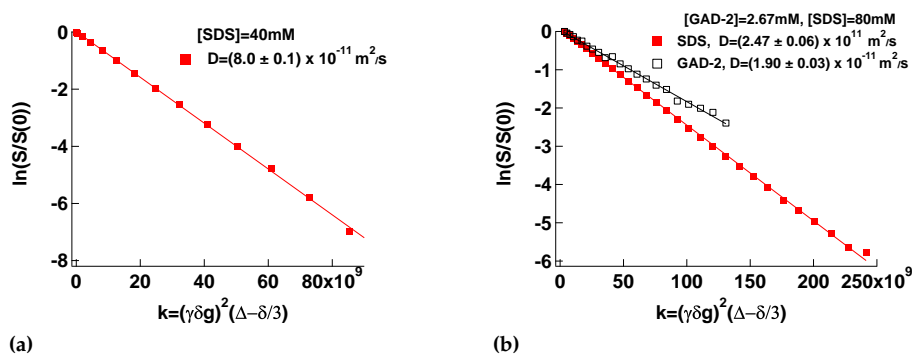


Fig. 2 The attenuation of the signal  $S(k)/S(0)$  on a log scale versus  $k = (\gamma\delta g)^2(\Delta - \delta/3)$  for (a) a peptide-free SDS sample with  $[\text{SDS}] = 40 \text{ mM}$  and  $0.1 \text{ M}$  sodium oxalate buffer (b) a GAD-2-SDS sample with  $[\text{SDS}] = 80 \text{ mM}$ ,  $[\text{GAD-2}] = 2.67 \text{ mM}$ , and  $0.1 \text{ M}$  sodium oxalate buffer.  $\delta = 2 \text{ ms}$  and  $\Delta = 100 \text{ ms}$ .

165 the signal attenuation of SDS was obtained by integrating the area under the spectral region  
 166 between 0 to 4 ppm. For the GAD-2-SDS system, the spectral ranges from 0 to 4 ppm and 7  
 167 to 9 ppm were used to obtain SDS and GAD-2 signal attenuation, respectively. In each case  
 168 the SDS and peptide spectral regions were chosen to ensure a clear spectral separation.

## 169 2.1 Relaxometry

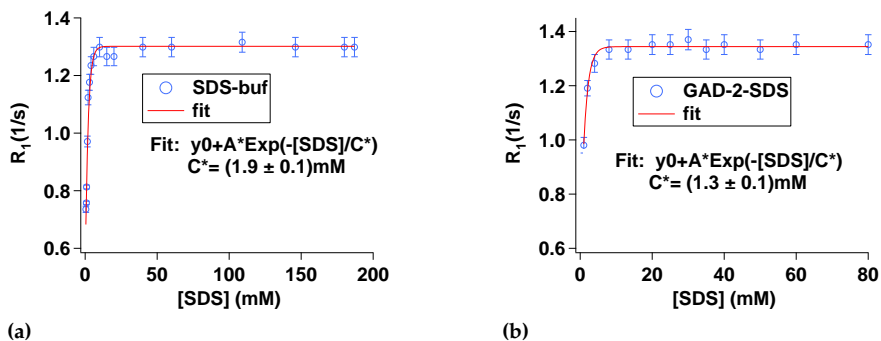


Fig. 3 Proton longitudinal relaxation rates  $R_1$  for SDS in (a) peptide-free SDS solutions versus SDS concentration  $[\text{SDS}]$ . (b) GAD-2-SDS solutions with  $R = [\text{SDS}]/[\text{GAD-2}] = 30$ . Similar measurements were carried out for the two dipeptides (not shown). The error bars represent the uncertainty in the numerical single exponential fit for the raw data of the relaxation time measurements.

170 Figure 3 shows the variation in the proton longitudinal relaxation rate  $R_1$  for the SDS  
171 peaks in peptide-free SDS solutions and GAD-2-SDS solution with increasing SDS con-  
172 centration. In all cases, the SDS concentration dependence can be fit to an exponential  
173  $y_0 + A \exp(-[SDS]/C^*)$ ; where  $C^*$  is identified as a characteristic SDS concentration that  
174 indicates a change in the local environment for the surfactant molecules in GAD-2-SDS  
175 and peptide-free systems.

176 The exponential fit yields a  $C^* = (1.9 \pm 0.1)$  mM for peptide-free SDS samples (figure 3a).  
177 For GAD-2-SDS samples, the spectral region from 0 to 4 ppm is used to calculate  $R_1$  for the  
178 SDS peaks at different SDS concentration. This yields a  $C^* = (1.3 \pm 0.1)$  mM (figure ??).

## 179 2.2 Diffusometry

### 180 2.2.1 Surfactant Solutions and Analysis Methods

181 Figure 4a shows the self-diffusion coefficient of SDS in 3 peptide-free SDS systems: one with  
182 sodium oxalate buffer with pH=4 (red open circles), and two without sodium oxalate buffer.  
183 Of the unbuffered solutions one was with pH unadjusted but measured to be between 3  
184 and 3.5 (blue open squares), and one with the pH=4 (black filled squares). Below  $[SDS]$   
185  $= 60$  mM, the SDS diffusion coefficient  $D_{Obs}^{SDS}$  for unbuffered solutions at different pH are  
186 indistinguishable from each other, while values in the buffered solution are much lower.

187 The pulsed-field-gradient signal attenuation is monoexponential for all samples (fig-  
188 ure 2). This implies that the exchange of SDS molecules between the SDS in micelles and  
189 in free solution is rapid in the NMR time scale. Previous studies (Soderman and Stilbs,  
190 1994) showed that a surfactant molecule visits more than one environment over very short  
191 timescales, and interpreted the observed diffusion coefficients using a two-site exchange  
192 model. In all the systems considered here, the SDS surfactant can either be a free monomer  
193 in solution or associated with a surfactant-rich aggregate. The observed self-diffusion coef-  
194 ficient of SDS is thus a linear combination of the self-diffusion coefficient  $D_{free}^{SDS}$  of the free  
195 molecules in bulk and that of the bound molecules in the micelle  $D_{micelle}^{SDS}$  in peptide-free  
196 solutions or a peptide-SDS complex  $D_{Aggr}^{SDS}$

$$\begin{aligned}
 D_{\text{Obs}}^{\text{SDS}} &= D_{\text{free}}^{\text{SDS}}, & [\text{SDS}] &\leq C_0, \\
 D_{\text{Obs}}^{\text{SDS}} &= (D_{\text{free}}^{\text{SDS}} - D_{\text{Aggr}}^{\text{SDS}})(f_s) + D_{\text{Aggr}}^{\text{SDS}}, & [\text{SDS}] &> C_0
 \end{aligned} \tag{2}$$

197 where  $f_s = [\text{SDS}]_{\text{free}}/[\text{SDS}]$  is the fraction of free SDS molecules,  $D_{\text{Aggr}}^{\text{SDS}}$  is either the micellar  
 198 diffusion coefficient in peptide-free samples, or the diffusion coefficient of the micelle-  
 199 peptide complex, and  $C_0$  refers to the critical (micellar or aggregation) concentration (CMC  
 200 or CAC), and  $[\text{SDS}]$  is the total SDS concentration. A key assumption of the model is that  
 201 there are only two distinct species, the free and the aggregate states; however, as will be  
 seen later, we are able to check for self-consistency of the model.

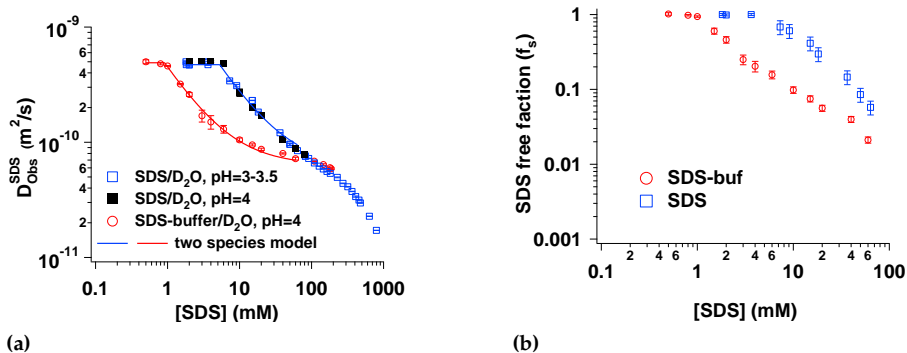


Fig. 4 Self-diffusion coefficient in peptide-free SDS solutions. (a)  $D$  versus SDS concentration  $[\text{SDS}]$  for solutions with sodium oxalate buffer (pH=4) (red open circles), and unbuffered, with pH=3-3.5 (blue open squares), and with pH=4 (black filled squares). (b) Fraction ( $f_s$ ) of free SDS with and without sodium oxalate buffer.

202

203 For simple spherical micelle systems, buffered and unbuffered peptide-free SDS solu-  
 204 tions,  $[\text{SDS}]_{\text{free}} = \text{CMC}$  for  $[\text{SDS}] > \text{CMC}$ . Therefore, equation 2 has 3 parameters,  $C_0 = \text{CMC}$ ,  
 205  $D_{\text{free}}^{\text{SDS}}$  and  $D_{\text{micelle}}^{\text{SDS}}$ . Fitting the buffered peptide-free SDS solution to the two-species model  
 206 in equation 2 yields the parameters  $D_{\text{free}}^{\text{SDS}} = (4.90 \pm 0.07) \times 10^{-10} \text{ m}^2/\text{s}$ ,  $D_{\text{micelle}}^{\text{SDS}} = (6.3 \pm 0.4)$   
 207  $\times 10^{-11} \text{ m}^2/\text{s}$ , and  $\text{CMC} = (0.91 \pm 0.02) \text{ mM}$ , while for the unbuffered peptide-free SDS solu-  
 208 tion  $D_{\text{free}}^{\text{SDS}} = (4.71 \pm 0.08) \times 10^{-10} \text{ m}^2/\text{s}$ ,  $D_{\text{micelle}}^{\text{SDS}} = (6.1 \pm 0.9) \times 10^{-11} \text{ m}^2/\text{s}$ , and  $\text{CMC} = (5.3 \pm 0.2) \text{ mM}$ .

209 The main physical insight hidden in these curves is the onset of crowding. While the  
 210 unbuffered and buffered solutions have very different dynamics at low [SDS], they converge  
 211 to the same value above 60 mM signifying a concentration where hydrodynamic interactions  
 212 between complexes slow down the dynamics and nullify the differences between aggregate  
 213 size. Such an effect of hydrodynamic interactions has indeed been previously noted (Ando  
 214 and Skolnick, 2010).

### 215 2.2.2 Peptide: GAD-2

When the size of a hydrophobic peptide is large enough that surfactant motion is rapid on the timescale of peptide motion, the peptide is expected to be associated with several surfactant molecules and there should never be free peptide, i.e. the peptide binding fraction is close to 1. For example, in the GAD-2–SDS system, since the concentration of SDS is 30 times higher than GAD-2 concentration ( $R = [\text{SDS}]/[\text{GAD} - 2] = 30$ ), we know that there is unlikely to be free peptide. In this case,  $D_{\text{Aggr}}^{\text{SDS}} = D^{\text{Peptide}}$ . Using this additional information allows us to use the two-site model even if the  $D_{\text{Obs}}^{\text{SDS}}$  versus  $1/[\text{SDS}]$  relationship is not linear. The only proviso is that the overall particulate volume fraction must always be small enough that hydrodynamic effects are negligible. For the peptide-free SDS system, we have seen that this is generally true for concentrations below 60 mM, or volume fractions below 0.04. For GAD-2–SDS system, the size of an GAD-2–SDS aggregate is expected to change with SDS concentration. Therefore, the concentration  $[\text{SDS}]_{\text{free}}$  of free SDS monomers is expected to change in the SDS concentration regime above CAC. We may simply rewrite and rearrange equation 2 for  $[\text{SDS}] > C_0$  but with  $D_{\text{Aggr}}^{\text{SDS}} = D^{\text{Peptide}}$ ,

$$f_s([\text{SDS}]) = \frac{[\text{SDS}]_{\text{free}}}{[\text{SDS}]} = \frac{D_{\text{Obs}}^{\text{SDS}} - D^{\text{Peptide}}}{D_{\text{free}}^{\text{SDS}} - D^{\text{Peptide}}}. \quad (3)$$

216 Figure 5a shows the self-diffusion coefficient of GAD-2 and SDS in the GAD-2–SDS  
 217 system. We measured the self-diffusion of GAD-2 in the SDS concentration range that is  
 218 higher than 13.3 mM. Due to experimental limitations (small value of signal-to-noise ratio),

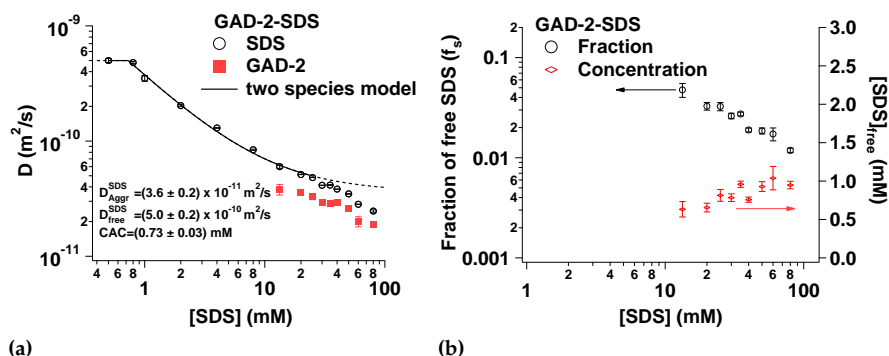


Fig. 5 (a) Self-diffusion coefficient of GAD-2 and SDS in a GAD-2-SDS system with  $R=[\text{SDS}]/[\text{GAD-2}]=30$  versus SDS concentration  $[\text{SDS}]$  (b) Fraction ( $f_s$ ) of free SDS and concentration ( $[\text{SDS}]_{\text{free}}$ ) of free SDS versus SDS concentration  $[\text{SDS}]$

219 we were not able to extract the self-diffusion coefficient of GAD-2 in the SDS concentration  
 220 range below 13.3 mM, but we were able to measure the surfactant diffusion.

221 The SDS self diffusion coefficient is fit well to the two species model for  $[\text{SDS}] \leq 25$   
 222 mM (figure 5a, solid line), and it deviates from the fit for higher SDS concentration (fig-  
 223 ure 5a, dotted line). The resulting fit parameters are  $D_{\text{free}}^{\text{SDS}} = (5.0 \pm 0.2) \times 10^{-10} \text{ m}^2/\text{s}$ ,  $D_{\text{Aggr}}^{\text{SDS}}$   
 224  $= (3.6 \pm 0.2) \times 10^{-11} \text{ m}^2/\text{s}$ , and  $\text{CAC} = (0.73 \pm 0.03) \text{ mM}$ .

225 PFG-NMR can be used to get spectrally-resolved diffusion coefficients. Using both SDS  
 226 and peptide diffusion coefficients as a function of  $[\text{SDS}]$ , we extract the fraction ( $f_s$ ) of free  
 227 surfactant in the monomer state in the aqueous solution as well as the concentration of free  
 228 surfactant  $[\text{SDS}]_{\text{free}}$ . This is shown in figure 5b. With increasing surfactant concentration,  
 229  $f_s$  decreases while  $[\text{SDS}]_{\text{free}}$  rises from 0.7 mM (close to the CAC) to  $\approx 1 \text{ mM}$  (close to  
 230 the CMC). This is consistent with the picture (Barhoum and Yethiraj, 2010; Jones, 2002)  
 231 that the concentration of free surfactant above the CAC/CMC is equal to the value of the  
 232 CAC/CMC. In the peptide-SDS system, and similar to the behavior in the nonionic polymer-  
 233 anionic surfactant (poly(ethylene)oxide-SDS) system (Barhoum and Yethiraj, 2010), the free  
 234 concentration rises further until it reaches the CMC value in the buffered solution.

Next, we estimate the hydrodynamic radius  $R_H$  of GAD-2-SDS complexes (figure 6a) using the Sutherland – Stokes – Einstein equation (Jones, 2002)

$$R_H = \frac{K_B T}{6\pi\eta D} \quad (4)$$

where  $K_B$  is the Boltzmann constant,  $T$  is the absolute temperature, and  $\eta$  is the solvent viscosity ( $\eta_{D_2O}=1.1$  mPa.s). The hydrodynamic radius  $R_H$  is obtained from the peptide diffusion ( $D = D^{\text{Peptide}}$ , open squares in figure 6a) as well as from the fitted value of  $D_{\text{Aggr}}^{\text{SDS}}$  obtained from the concentration dependence of the surfactant diffusion (dashed red line in figure 6a). For  $[\text{SDS}] < 25$  mM the hydrodynamic radii obtained via peptide diffusion and surfactant diffusion are roughly the same, with a value of approximately 5.5 nm. Interestingly,  $R_H$  (obtained from peptide diffusion  $D^{\text{Peptide}}$ ) increases as a function of SDS concentration to about 10 nm at 60 mM, less than a factor of two increase.

Plotted in figure 6b is the variation in the ratio of SDS molecules to peptide molecules in a complex  $r = ([\text{SDS}] - [\text{SDS}]_{\text{free}})/([\text{SDS}]/R) = (1 - f_s) R$  exhibits a very slight increase, from  $\approx 28$  to 29, and approaches  $R = 30$  asymptotically. We need to understand how the aggregate size changes in order to accommodate the two-fold increase in the hydrodynamic radius  $R_H$ ; we will return to this point later.

### 2.2.3 Comparison with smaller dipeptides

In order to study the effect of peptide size on the dynamics of peptide-SDS complexes, diffusometry was carried out to quantify complex formation of SDS with the dipeptides Ala-Gly and Tyr-Leu.

A plot of the SDS self-diffusion coefficient for all systems in the current study in one graph (figure 7) shows clearly that SDS diffusion looks similar for the systems with small di-peptides (Ala-Gly and Tyr-Leu) and the peptide-free SDS system with sodium oxalate buffer. This suggests that the fraction of free SDS in the Tyr-Leu-SDS and Ala-Gly-SDS systems is similar to the fraction of free SDS in the peptide-free SDS system with buffer (figure 4b). On the other hand, SDS diffusion looks very different for the system with

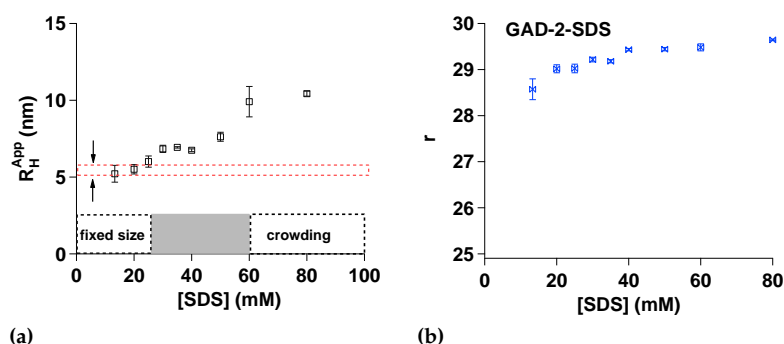


**Fig. 6** (a) The apparent hydrodynamic radius ( $R_H^{\text{APP}}$ ), extracted from the peptide diffusion coefficient, of GAD-2-SDS complexes versus SDS concentration [SDS]. The horizontal dashed line is the value of apparent hydrodynamic radius ( $R_H^{\text{APP}} = 5.5 \pm 0.3$  nm) obtained *via* the SDS aggregate diffusion coefficient ( $D_{\text{Aggr}}^{\text{SDS}} = (3.6 \pm 0.2) \times 10^{-11}$  m<sup>2</sup>/s) at low SDS concentration [SDS]  $\leq 25$  mM, where the two species model is valid. This value is in agreement with the peptide diffusion coefficient. At high SDS concentration [SDS]  $\geq 60$  mM. The diffusion coefficient measured gives no information about the true hydrodynamic radius. The intermediate SDS concentration regime, denoted by the gray area, is the regime in which either complex size is indeed increasing with concentration or hydrodynamic interactions between complexes is slowing down the motions. (b) The ratio of SDS molecules to peptide molecules in a complex ( $r$ ) versus SDS concentration ([SDS]) for GAD-2-SDS samples.

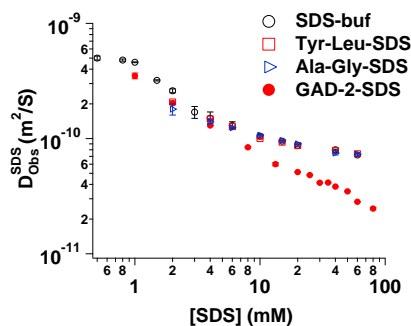


**Fig. 7** Self-diffusion coefficient of SDS in all the systems studied: peptide-free SDS system with sodium oxalate buffer, Tyr-Leu-SDS, Ala-Gly-SDS, and GAD-2-SDS with  $R = [\text{SDS}]/[\text{GAD-2}] = 30$  samples.

258 long peptide (GAD-2-SDS system), suggesting that the GAD-2-SDS complexes are very  
 259 different from the Ala-Gly-SDS and Tyr-Leu-SDS complexes, which are essentially indis-  
 260 tinguishable from micellar aggregates with no peptide. This means that the peptide-micelle  
 261 binding characteristics of the Tyr-Leu and Ala-Gly dipeptides are different from the much  
 262 longer GAD-2 peptide. Also, this indicates that GAD-2 significantly disrupts the micellar  
 263 aggregate. This conclusion likely extends to other long and hydrophobic peptides.

### 264 3 Conclusion

265 NMR-based techniques have been utilized in this work to study the nature of peptide-  
266 micelle complexes in a buffered 19-residue antimicrobial peptide (the GAD-2-SDS system).  
267 First, we examined the impact of the buffer (figure 4a). Varying the pH over a small range  
268 in the absence of a buffer shows no effect on the micellar structure, while the CMC is lower  
269 in the presence of the buffer.

270 At high surfactant concentrations ( $[SDS] > 60$  mM), the observed diffusion coefficients  
271 of surfactant SDS molecules merge for buffered and unbuffered peptide-free SDS systems.  
272 In addition, the linear two species model (equation 2), is valid below  $[SDS]=60$  mM but  
273 not valid above. This is similar to the findings in previous work for a system of anionic  
274 surfactant (SDS)-nonionic polymer polyethylene oxide (PEO) (Barhoum and Yethiraj, 2010)  
275 where this concentration was identified as the onset of macromolecular crowding: this  
276 refers to the excluded volume effect of one macromolecule with respect to another (Zhou  
277 et al, 2008). Our primary finding is that  $[SDS]=60$  mM signals the concentration beyond  
278 which one cannot, even in principle, extract hydrodynamic radii or aggregate ratios.

279 At low surfactant concentrations ( $[SDS] < 25$  mM), the observed diffusion coefficient of  
280 SDS (figure 5a) is well described by the two-species model in equation 2. Moreover, in this  
281 range, the surfactant aggregate diffusion coefficient and the peptide diffusion coefficient  
282 coincide. This is a self-consistency check that gives confidence in the linear two species  
283 model and the results obtained.

284 At intermediate SDS concentrations, the apparent hydrodynamic size increases from 5.5  
285 nm at 25 mM to 10 nm at 60 mM (figure 6a). This increase in the apparent hydrodynamic  
286 size might either reflect a true increase in aggregate size, or it might indicate the existence  
287 of hydrodynamic interactions between complexes. Given that the ratio of SDS to GAD-  
288 2 molecules in a complex is not changing by much, i.e.  $r \approx R$  (figure 6b), an increase in  
289 the mean aggregate size might arise from an increase in the average number of peptides  
290 in one complex from 1 (at 25 mM) to approximately 2 (at 60 mM). A third possibility is  
291 that such an increase in hydrodynamic radius arises from a change in shape (for example

292 from spherical to oblate or prolate) (Bloomfield, 2000). However, in order to account for  
 293 a factor two increase, one would need to have a rather spectacular shape change with  
 294 a formation of very anisotropic complexes with an approximately 20:1 axial ratio. These  
 295 three possibilities - an increase in number of peptides in a complex, long-range interactions  
 296 between complexes, or a dramatic change in complex shape - are depicted in figure 8.  
 297 As noted by (Zhou et al, 2008; Schreiber et al, 2009), a deeper understanding of role of  
 298 electrostatic and hydrodynamic interactions is needed in the study of macromolecular  
 299 crowding, and this needs to be studied further.

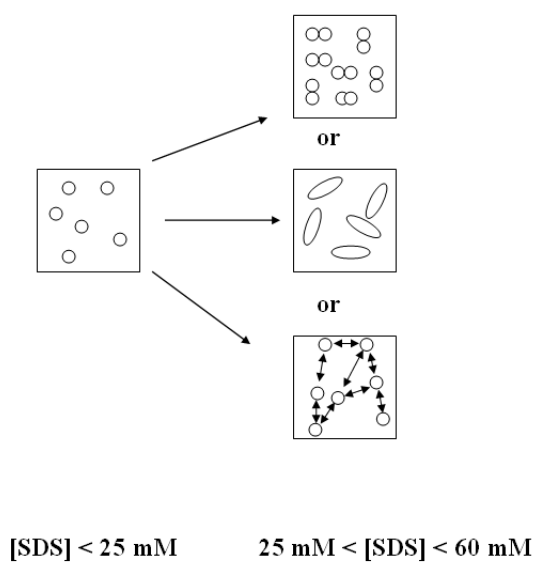


**Fig. 8** A schematic diagram showing each peptide-surfactant complex as a single isolated complex (left, isolated circles) at low SDS concentrations. Results at intermediate SDS concentrations are consistent with either two peptides in each complex schematically represented by two circles (top right), highly anisotropic complexes (right middle), or long-range hydrodynamic interactions represented by arrows between complexes (right bottom).

300 There is a distinct difference in the behavior of large peptides ( $M_w^{\text{peptide}} > M_w^{\text{surfactant}}$ ) and  
 301 small dipeptides ( $M_w^{\text{peptide}} \approx M_w^{\text{surfactant}}$ ). The small dipeptides (Ala-Gly and Tyr-Leu) hardly  
 302 affect the SDS diffusion coefficient (figure 7). This indicates that the dipeptides behave just  
 303 as the surfactant does: i.e. rapidly exchanging between aggregate and free state. For large  
 304 peptides such as GAD-2, on the other hand, rapid exchange between free and aggregate

305 state is practically impossible. This is because the surfactant molecules form micellar-like  
306 aggregates along the peptide chain, consistent with a bead-on-a-chain picture (Chari et al,  
307 2004; Roscigno et al, 2003) for large-molecule aggregates. We therefore expect the approach  
308 outlined in this work to be valid generally for large hydrophobic peptides.

309 As a conclusion, some recommendations are suggested in order to extract parameters  
310 such as the hydrodynamic radius and peptide binding fractions. All our results consistently  
311 show that measurements should be made well below the concentration that signals the onset  
312 of crowding (about 60 mM for SDS). Furthermore, even at intermediate concentrations, the  
313 true hydrodynamic size of the peptide-SDS complex is not necessarily constant, and the  
314 concentration dependence of the hydrodynamic radius can still not be ignored. The only  
315 unambiguous concentration-independent statements can be made at low concentrations:  
316 in this system, this is below [SDS]= 25 mM.

#### 317 **4 Acknowledgments**

318 All the authors acknowledge financial support from the National Science and Engineering  
319 Research Council of Canada (NSERC). We also acknowledge useful suggestions from Carl  
320 Michal (University of British Columbia) and Ivan Saika-Voivod (Memorial University of  
321 Newfoundland).

#### 322 **References**

- 323 Andersson A, Almqvist J, Hagn F, Maler L (2004) Diffusion and dynamics of penetratin in  
324 different membrane mimicking media. *Biochim Biophys Acta* 61:18–25
- 325 Ando T, Skolnick J (2010) Crowding and hydrodynamic interactions likely dominate in  
326 vivo macromolecular motion. *PNAS* 107:18,457–18,462
- 327 Barhoum S, Yethiraj A (2010) An NMR study of macromolecular aggregation in a model  
328 polymer-surfactant solution. *J Chem Phys* 132:1–9
- 329 Batchelor GK (1976) Brownian diffusion of particles with hydrodynamic interaction. *J Fluid*  
330 *Mech* 74:1–29

- 331 Begotka BA, Hunsader JL, Oparaache C, Vincent JK, Morris KF (2006) A pulsed field  
332 gradient NMR diffusion investigation of enkephalin peptide-sodium dodecyl sulfate  
333 micelle association. *Magn Reson Chem* 44:586–593
- 334 Binks BP, Chatenay D, Nicot C, Urbach W, Waks M (1989) Structural parameters of the  
335 myelin transmembrane proteolipid in reverse micelles. *Biophys J* 55:949–955
- 336 Bloomfield VA (2000) Survey of Biomolecular Hydrodynamics. In: Separations and Hydro-  
337 dynamics.(Todd M. Schuster, editor). On-Line Biophysics Textbook, Biophysics society,  
338 [www.biophysics.org](http://www.biophysics.org)
- 339 Browne MJ, Feng CY, Booth V, Rise ML (2011) Characterization and expression studies of  
340 gaduscidin-1 and gaduscidin-2; paralogous antimicrobial peptide-like transcripts from  
341 atlantic cod (*gadus morhua*). *Dev Comp Immunol* 35:399–408
- 342 Buchko GW, Rozek A, Hoyt DW, Cushley RJ, Kennedy MA (1998) The use of sodium dodecyl  
343 sulfate to model the apolipoprotein environment. evidence for peptide SDS complexes  
344 using pulsed-field-gradient NMR spectroscopy. *Biochim Biophys Acta* 1392:101–108
- 345 Chari K, Kowalczyk J, Lal J (2004) Conformation of poly(ethylene oxide) in polymer-  
346 surfactant aggregates. *J Phys Chem B* 108:2857–2861
- 347 Chatterjee C, Majumder B, Mukhopadhyay C (2004) Pulsed-field gradient and saturation  
348 transfer difference NMR study of enkephalins in the ganglioside GM1 micelle. *J Phys*  
349 *Chem B* 108:7430–7436
- 350 Chinchar V, Bryan L, Silphadaung U, Noga E, Wade D, Rollins-Smith L (2004) Inactivation of  
351 viruses infecting ectothermic animals by amphibian and piscine antimicrobial peptides.  
352 *J Virol* 323:268–275
- 353 Cozzolino S, Sanna MG, Valentini M (2008) Probing interactions by means of pulsed field  
354 gradient nuclear magnetic resonance spectroscopy. *Magn Reson Chem* 46:S16S23
- 355 Deaton KR, Feyen EA, Nkulabi HJ, Morris KF (2001) Pulsed-field gradient NMR study of  
356 sodium dodecyl sulfate micelle-peptide association. *Magn Reson Chem* 39:276–282
- 357 Epand RM, Vogel HJ (1999) Diversity of antimicrobial peptides and their mechanisms of  
358 action. *Biochim Biophys Acta* 1462:11–28

- 359 Fernandes JMO, Ruangsri J, Kiron V (2010) Atlantic cod piscidin and its diversification  
360 through positive selection. *Public Library of Science* 5:1–7
- 361 Gao X, Wong TC (1998) Studies of the binding and structure of adrenocorticotropin peptides  
362 in membrane mimics by NMR spectroscopy and pulsed-field gradient diffusion. *Biophys*  
363 *J* 75:1871–1888
- 364 Gimel JC, Brown W (1996) A light scattering investigation of the sodium dodecyl sul-  
365 fatelysozyme system. *J Chem Phys* 104:8112–8117
- 366 Hoskin DW, Ramamoorthy A (2008) Studies on anticancer activities of antimicrobial pep-  
367 tides. *Biochim Biophys Acta* 1778:357–375
- 368 Jones JA, Wilkins DK, Smith LJ, Dobson CM (1997) Characterisation of protein unfolding  
369 by NMR diffusion measurements. *J Biomol NMR* 10:199–203
- 370 Jones RAL (2002) *Soft Condensed Matter*, 1st edn. Oxford University Press Inc, New York
- 371 Morein S, Trouard TP, Hauksson JB, Rilfors U, Arvidson G, Lindblom G (1996) Two-  
372 dimensional  $^1\text{H}$ -NMR of transmembrane peptides from *escherichia coli* phosphatidyl-  
373 glycerophosphate synthase in micelles. *Eur J Biochem* 241:489–497
- 374 Nicolas P (2009) Multifunctional host defense peptides: intracellular-targeting antimicrobial  
375 peptides. *Federation of European Biochemical Societies* 276:6483–6496
- 376 Orfi L, Lin M, Larive CK (1998) Measurement of SDS micelle-peptide association using  $^1\text{H}$   
377 NMR chemical shift analysis and pulsed-field gradient nmr spectroscopy. *J Anal Chem*  
378 + 70:1339–1345
- 379 Price WS (1997) Pulsed-field gradient nuclear magnetic resonance as a tool for studying  
380 translational diffusion: Part I. basic theory. *Concept Magnetic Res* 9:299–336
- 381 Qureshi T, Goto NK (2012) Contemporary methods in structure determination of membrane  
382 proteins by solution NMR. *Top Curr Chem* 326:123–185
- 383 Rege K, Patel SJ, Megeed Z, Yarmush ML (2007) Amphipathic peptide-based fusion peptides  
384 and immunoconjugates for the targeted ablation of prostate cancer cells. *Cancer Research*  
385 *Journal* 67:6368–2375
- 386 Romani AP, Marquezina CA, Ito AS (2010) Fluorescence spectroscopy of small peptides  
387 interacting with microheterogeneous micelles. *Int J Pharm* 383:154–156

- 388 Roscigno P, Asaro F, Pellizer G, Ortona O, Paduano L (2003) Complex formation between  
389 poly(vinylpyrrolidone) and sodium decyl sulfate studied through NMR. *J Am Chem Soc*  
390 119:9639–9644
- 391 Ruangsri J, Salger SA, Caipang CM, Kiron V, Fernandes JM (2012) Differential expression  
392 and biological activity of two piscidin paralogues and a novel splice variant in atlantic  
393 cod (*Gadus morhua* L.). *Fish Shellfish Immun* 32:396–406
- 394 Sanders CR, Sönnichsen F (2006) Solution NMR of membrane proteins: practice and chal-  
395 lenges. *Magn Reson Chem* 44:s24–s40
- 396 Sarker M, Rose J, McDonald M, Morrow MR, Booth V (2011) Modifications to surfactant  
397 protein b structure and lipid interactions under respiratory distress conditions: Conse-  
398 quences of tryptophan oxidation. *J Biomol NMR* 50:25–36
- 399 Schreiber G, Haran G, Zhou HX (2009) Fundamental aspects of protein-protein association  
400 kinetics. *Chem Rev* 109:839–860
- 401 Soderman O, Stilbs P (1994) NMR studies of complex surfactant systems. *Prog Nucl Mag*  
402 *Res Sp* 26:445–482
- 403 Tulumello DV, Deber CM (2009) SDS micelles as a membrane-mimetic environment for  
404 transmembrane segments. *J Biochem* 48:12,096–12,103
- 405 Wang G (1999) Structural biology of antimicrobial peptides by NMR spectroscopy. *Curr*  
406 *Org Chem* 10:569–581
- 407 Wang G (2008) NMR studies of a model antimicrobial peptide in the micelles of SDS, dode-  
408 cylphosphocholine, or dioctanoylphosphatidylglycerol. *The Open Magnetic Resonance*  
409 *Journal* 1:9–15
- 410 Whitehead TL, Jones LM, Hicks RP (2001) Effects of the incorporation of CHAPS into  
411 SDS micelles on neuropeptide-micelle binding: Separation of the role of electrostatic  
412 interactions from hydrophobic interactions. *Biopolymers* 58:593–605
- 413 Whitehead TL, Jones LM, Hicks RP (2004) PFG-NMR investigations of the binding of  
414 cationic neuropeptides to anionic and zwitterionic micelles. *J Biomol Struct Dyn* 21:567–  
415 576

- 416 Yu L, Tan M, Ho B, Ding JL, Wohland T (2006) Determination of critical micelle concentra-  
417 tions and aggregation numbers by fluorescence correlation spectroscopy: Aggregation of  
418 a lipopolysaccharide. *Anal Chim Acta* 556:216–225
- 419 Zasloff M (2002) Antimicrobial peptides of multicellular organisms. *Nature* 415:389–395
- 420 Zhou HX, Rivas G, , Minton AP (2008) Macromolecular crowding and confinement: bio-  
421 chemical, biophysical, and potential physiological consequences. *Annu Rev Biophys*  
422 37:375–397